ELSEVIER

Biophysical Chemistry 67 (1997) 245–261

Biophysical Chemistry

Free energy of the binding of uridylic acid oligomers with double stranded poly(A) · poly(U)

E. Raukas [a,*], K. Kooli [a], V.I. Yamkovoi [b], H. Schütz [c,1]

[a] *Institute of Experimental Biology of Estonian Academy of Sciences, Harku EE3051, Estonia*
[b] *Novosibirsk State University, 630090 Novosibirsk, Russia*
[c] *Institut für Molekularbiologie, Friedrich-Schiller-Universität, Winzerlaer Strasse 10, D-07745 Jena, Germany*

Received 10 March 1997; accepted 25 March 1997

Abstract

The binding parameters (K, ω) and the free energy (ΔG^0) of triple helix formation have been estimated for complexes of oligo(U)$_n$ ($n = 5$, 7–10) with poly(A) · poly(U) on the basis of hypochromicity measurements. The data were treated according to the formula of McGhee and von Hippel [J. Mol. Biol. 86 (1974) 469] by a computer program ALAU [H. Schütz et al., Stud. Biophys. 104 (1984) 23] which takes absorbancies and total concentrations as input. In 1 mM cacodylate buffer pH 7.0 with 10 mM NaCl and 10 mM $MgCl_2$ at 5°C the free energy of contiguous binding was found to be a linear function of the oligomer length with a slope of $\Delta G^0_{c,U} = -0.72$ (± 0.03) kcal · mol^{-1} per nucleotide. The mean cooperativity coefficient (ω) was 24.5 (± 5.6), and the corresponding free energy of interaction between the neighbouring oligonucleotides in the third strand was $\Delta G^{0}_{\omega} = -1.74$ (± 0.13) kcal · mol^{-1}. © 1997 Elsevier Science B.V.

Keywords: Oligouridylic acid; Interaction with poly(A) · poly(U); Thermodynamic parameters; Free energy; Binding parameters; UV spectrophotometry

1. Introduction

Recently, a wide renewal of interest in the triple helix (H-form of DNA) has occurred resulting from the assumed role of this specific structure in cellular activity [1–3]. Synthetic oligonucleotides have been shown to form local triple helices with polypurine/polypyrimidine sequences in DNA and could therefore be applied to control the biosynthetic processes of the cell [4–6]. Reviews on the structure and physicochemical properties of the triple helix have been published [7–9]. The important role assigned to the triple helical regions of the cellular DNA have made it urgent to determine the physical properties of this very special conformation of nucleic acids.

It is known that ribopolymers form triple helices as well [10–12]. From the experiments with polynucleotides it has been concluded that triple helices may be formed either solely of RNA strands or of both RNA and DNA strands in different combinations. Double stranded deoxypolynucleotides could be used to bind RNA homopolymers and oligomers

* Corresponding author. E-mail: ergo@ebi.estnet.ee

[1] Part of the work was done while H.S. belonged to the Institut für Molekulare Biotechnologie e.V., Department of Structural Biology – Crystallography, Beutenbergstrasse 11, D-07745 Jena, Germany.

PII S0301-4622(97)00043-4

[13–15]. Depending on the type of the polynucleotide (RNA or DNA) involved and the position of the given strand in the triplet as well as environmental conditions, the triple helices consisting of both RNA and DNA strands may be of quite different stability. These data have been confirmed by experiments with triple helices formed by oligonucleotides containing A/dA and G/dG in the purine strand, and U/T and C/dC in the two pyrimidine strands. Among the eight possible combinations of RNA and DNA strands in a triplex, the highest stability of the Hoogsten paired third strand was found in the case of a RNA strand being bound either to DNA/DNA [16–18] or to DNA/RNA [19] (resp. purine/pyrimidine) double helices.

The high stability of triple helices containing uridylic acid oligomers as a third strand would be unexpected per se since the lack of the methyl group (as compared with thymidine) is known to reduce the stacking energy of the base. Hence, the preferred stabilization of RNA strands in the Hoogsten position is entirely due to backbone conformational preference which facilitates the interaction of 2′-OH ribose groups with the phosphate groups of the purine strand [16,20], i.e., the oligoribonucleotides have distinct preference over oligodeoxynucleotides as candidates for the third strand in a triplex. Due to the higher stability of RNA-containing triplexes, the question about the structure and stability of RNA strands in Hoogsten pairing is also of interest with regard to applications [21]. Pyrimidine containing oligomers of the RNA type have proved to be more effective in repression of bacteriophage T7 polymerase initiation in vitro as compared with DNA oligomers [22].

A number of investigators have used UV melting and van't Hoff's method to obtain thermodynamic data for triple helices of different types. However, the methods based upon the melting temperature of the complexes have frequently resulted in biased values for enthalpy as well as for free energy [8,23]. Besides, most of the experiments have been performed with oligonucleotides containing both dT (U) and dC (C) in different proportions which do not enable one to calculate the values for specific nucleotides. Free energy has frequently been determined as the difference between enthalpic and entropic terms, resulting in a relatively large error.

We report herein changes in the free energy of uridylic acid residues upon interaction with an RNA double helix making use of hypochromicities. The binding of short oligoribonucleotides $(pU)_n$ ($n = 5$–10) with double stranded ribopolymer poly(A) · poly(U) at 5°C was studied. The differences between absorbance measured at 260 nm upon complex formation at 5°C and the absorbance determined for the fully dissociated state at higher temperatures were used to calculate the binding parameters.

2. Materials and methods

2.1. Materials

Poly(A) · poly(U) from Serva or Vector (Novosibirsk) was used. Occasionally, poly(A) · poly(U) was annealed at room temperature in 10 mM sodium cacodylate (pH 7.0), 30 mM NaCl, using poly(A) and poly(U) from Serva. The solution was thoroughly dialysed against 1 mM cacodylate buffer pH 7.0 containing 10 mM NaCl. Stock solutions of uridylic acid oligomers were prepared in the same buffer.

Molecular mass of the polymers was determined by electrophoresis in 1% agarose gel. The specimens were run in 40 mM Tris acetate buffer containing 1 mM EDTA (pH 8.0), gels were stained with methylene blue. The degree of polymerization of poly(A) and poly(U) were found to be in the range 200–500 and 200–300, respectively. The molecular mass of the poly(A) · poly(U) specimens was estimated to be in the range 50–500 bp.

Ribonucleic acid oligomers $(pU)_n$ ($n = 3 - 10$) and $(pA)_{12}$ were prepared by hydrolysis of poly(U) and poly(A) (Vector) respectively, with RNase from venom of *Naja oxiana* [24]. The reaction was carried out in a solution containing both 50 mM NaCl and 10 mM $MgCl_2$ at 30°C. Oligonucleotides were fractionized on a QAE-Sephadex A-25 column in the gradient of ammonium bicarbonate (pH 8.6) in presence of 15% dioxane.

2.2. Determination of concentrations

The following extinction coefficients were adopted for the determination of concentrations at room tem-

perature: $\epsilon_{260} = 6655\ l \cdot mol^{-1} \cdot cm^{-1}$ for poly(A) · poly(U) in 10 mM NaCl solution, $\epsilon_{257} = 10\,000\ l \cdot mol^{-1} \cdot cm^{-1}$ for poly(A), $\epsilon_{261} = 9300\ l \cdot mol^{-1} \cdot cm^{-1}$ for poly(U), $\epsilon_{261} = 9500, 9400, 9300\ l \cdot mol^{-1} \cdot cm^{-1}$ for $(pU)_n$ ($n = 3,4$, $n = 5,6$, $n = 7–10$, respectively), and $\epsilon_{257} = 10\,800\ l \cdot mol^{-1} \cdot cm^{-1}$ for $(pA)_{12}$ [25]. These values have been corrected in order to calculate the absorbances at lower temperatures and in presence of Mg^{2+} (see Eqs. (1) and (2), Section 2.5). Unless stated otherwise, all extinction coefficients given here and below refer to phosphorus concentration.

2.3. Preparation of complexes

In order to favour the triple helix formation, all experiments were carried out in the presence of 10 mM Mg^{2+}. The standard solution used was 1 mM cacodylate buffer, pH 7.0, containing both 10 mM NaCl and 10 mM Mg^{2+} (CNM buffer), if not stated otherwise. The complexes were prepared and measured one by one for each of the ratios $r = [P^-]_{oligo(U)}/[P^-]_{poly(A\cdot U)}$, no titration of the initial solution in series was used.

The complexes were prepared directly in the spectrophotometric cuvettes using magnetic stirring. Stoppered cuvettes were used; the smaller cuvettes were covered with parafilm during the measurements to avoid evaporation. The level of the solution in the cuvettes was hold low enough to prevent accidental moistening of the cuvette opening and subsequent loss of some solution when the cuvettes were closed with stopper or parafilm (or opened again) during the weighing and measurement cycles.

Our preliminary experiments had shown that the addition of Mg^{2+} to poly(A) · poly(U) solution results in a change of absorbance in the 260 nm band (see Section 3) a prolonged storage or heating of the solution in the premelting region in the presence of Mg^{2+} results in an additional small change of the spectrum. The absorbance change at 320 nm was negligible. Therefore, in order to minimize the effect of Mg^{2+} ions upon poly(A) · poly(U) during the preparation and measurements, $MgCl_2$ was added at the very end of the sample preparation.

The following succession of preparation steps was maintained. First, the absorbance of the buffer solution was determined at 260 and 320 nm. Thereafter, the buffer solution was removed and the cuvette was filled again with a smaller portion of fresh buffer; poly(A) · poly(U) was added to the buffer solution, being continuously stirred. The initial concentration of the polymer solution was determined at 260 nm, using $\epsilon_{260} = 6655\ l \cdot mol^{-1} \cdot cm^{-1}$, and recalculated in accordance with the dilution. Next, the oligonucleotide solution was added, and finally, the solution was adjusted to 10 mM Mg^{2+} with 0.1 M (or 1 M) $MgCl_2$. After each step, (i) the volume of the solution was checked using analytical balances (readings were corrected for the density of the solution), and (ii) all the absorbance values were read both at 260 and 320 nm; the latter values were used to correct the readings at 260 nm. Respective concentrations of ingredients were calculated according to the dilution.

2.4. Measurements

UV spectra were recorded on a Pye-Unicam SP8-150 spectrophotometer. The spectrophotometer was connected to a personal computer provided with a special program to read the digital results and to perform the calculations. The single beam mode was applied for spectrophotometric measurements using the concentration scale of the instrument (four digits).

First, the dependence of buffer absorbance on wavelength was recorded against air. Also all other spectra were recorded against air and corrected digitally for buffer absorbance in the same cuvette, as well as for the shift of zero line at 320 nm.

After the measurement of the buffer spectrum, the poly(A) · poly(U) solution as well as the complex were prepared in the same cuvette (as described in Section 2.3) and placed into the sample beam of the instrument. The spectra were recorded in 1 nm steps within the interval of 320 to 220 nm; the averages of five readings at each wavelength were registered.

In order to follow the hysteresis of the melting curves the spectra of the mixtures of oligo(U) and poly(A) · poly(U) were recorded in the following order: (i) at room temperature, (ii) at 33 or (in some series) at 45°C, (iii) at 5°C, and (iv), at the temperature corresponding to complete dissociation of the complex (20, 33 or 45°C), again. Melting curves were followed during the temperature change. In order to prevent the modification of the poly(A) ·

poly(U) at higher temperature by Mg^{2+} ions, the first heating cycle was not regularly used.

To avoid the condensation of water vapour on the cell walls and lenses during the cooling cycle, an open dish with phosphorus pentoxide was placed in the cuvette compartment, and the compartment was provided with a supplementary cover.

2.5. Absorbance correction and calculation of differences

Poly(A) · poly(U), poly(A) and poly(U) undergo conformational transitions when ionic conditions and/or temperature are changed. Therefore, all components were also studied separately.

All spectra were standardized so that the absorbance at 320 nm always equalled zero (zero shift). Absorbances corrected according to light scattering rules did not result in any improvement.

The absorbance difference accompanying the complex formation was found via two different methods. In the first case, the absorbance difference at 260 nm between two states, i.e., at 5°C (1°C in the case of pentauridylates) and at 20, 33 or 45°C (complete dissociation) was used. The differences were corrected for the small changes of poly(A) · poly(U) and oligo(U) absorbances measured in the presence of Mg^{2+} in the same range of temperatures ($\Delta\epsilon''_{AU,260} = -30$, -100, or -230 $l \cdot mol^{-1} \cdot cm^{-1}$ and $\Delta\epsilon''_{U,260} = -55$, -65, or -50 $l \cdot mol^{-1} \cdot cm^{-1}$, respectively) according to

$$\Delta A_{260} = A_{260}(5°C) - A_{260}(t°C) - (\Delta\epsilon''_{AU,260} \cdot c_{AU,t} + \Delta\epsilon''_{U,260} \cdot c_{U,t}) \quad (1)$$

where $c_{AU,t}$ and $c_{U,t}$ are total concentrations of poly(A) · poly(U) and $(pU)_n$, respectively, expressed on the basis of phosphorus. The absorbance change due to the temperature dependence of the solution density was taken into account by the same coefficients.

The other way to estimate the absorbance difference was to calculate the expected value of absorbance at 5°C, $A_{260}(5°C)$, using the known concentrations of poly(A) · poly(U) and $(pU)_n$ and the extinction coefficients at room temperature with no Mg^{2+} ions present (Eq. (2), first line), and to correct it for the absorbance change resulting from the addition of Mg^{2+} and cooling of the solution from 20°C to 5°C (second and third lines):

$$\Delta A_{260} = A_{260}(5°C) - (\epsilon_{AU,260} \cdot c_{AU,t} + \epsilon_{U,260} \cdot c_{U,t}) - (\Delta\epsilon'_{AU,260} \cdot c_{AU,t} + \Delta\epsilon'_{U,260} \cdot c_{U,t}) - (\Delta\epsilon''_{AU,260} \cdot c_{AU,t} + \Delta\epsilon''_{U,260} \cdot c_{U,t}) \quad (2)$$

where subscripts AU and U refer to poly(A) · poly(U) and $(pU)_n$, respectively; $\Delta\epsilon'_{AU,260} = -165$ $l \cdot mol^{-1} \cdot cm^{-1}$ and $\Delta\epsilon'_{U,260} = +10$ $l \cdot mol^{-1} \cdot cm^{-1}$ are the respective extinction increments due to addition of Mg^{2+} at room temperature, $\Delta\epsilon''_{AU,260} = -30$ $l \cdot mol^{-1} \cdot cm^{-1}$ and $\Delta\epsilon''_{U,260} = -55$ $l \cdot mol^{-1} \cdot cm^{-1}$ are those due to the cooling. The resulting values $\epsilon_{AU,260}(5°C) = 6480$ $l \cdot mol^{-1} \cdot cm^{-1}$ and $\epsilon_{U,260}(5°C) = 9355$ (resp. 9255) $l \cdot mol^{-1} \cdot cm^{-1}$ were applied to calculate the expected absorbances in 10 mM Mg^{2+} at 5°C for poly(A) · poly(U) complexes with $(pU)_n$ $n = 5,6$, and $n = 7–10$.

Both the difference between the experimental and theoretical values of absorbance at 5°C (Eq. (2)) and absorbance differences on the melting curves (Eq. (1)) were employed to calculate the concentration of bound ligand. However, better fits of the data upon calculation of binding parameters were obtained using Eq. (1).

2.6. Multiple wavelengths measurements

Preliminary experiments revealed that the melting of poly(A) · poly(U) in presence of 10 mM $MgCl_2$ is characterized by a decrease of absorbance at 280 nm in the range of 20–30°C, pointing to possible involvement of the disproportionation reaction

$$2\text{poly(A)} \cdot \text{poly(U)} \rightarrow \text{poly(A)} \cdot 2\text{poly(U)} + \text{poly(A)} \quad (a)$$

In order to study the disproportionation more closely the temperature dependence of absorbance was recorded at several wavelengths in the region 260–320 nm.

For treatment of experimental data the difference spectra of the transitions

$$\text{poly(A)} + \text{poly(U)} \rightarrow \text{poly(A)} \cdot \text{poly(U)} \quad (b)$$

$$\text{poly(A)} \cdot \text{poly(U)} + \text{poly(U)} \rightarrow \text{poly(A)} \cdot 2\text{poly(U)} \quad (c)$$

were determined at room temperature after 4–7 days of mixing the components. The spectrum accompanying the disproportionation (a) was found as a difference between the spectra of transitions (c) and (b).

The melting of the complex poly(A) · poly(U) + $(pU)_n$ was considered to consist of two simultaneous reactions: dissociation of uridine oligomers from double helical poly(A) · poly(U) and disproportionation of double helix. The first reaction could be revealed by the presence of a difference spectrum (c) with opposite sign, whereas the occurrence of disproportionation could be shown on the basis of the difference spectrum (a) in the experimental spectra.

As a result of reaction (a) half of the poly(A) present in double helix becomes free to react with Mg^{2+}. However, due to the likeness between the difference spectra (b) and spectrum of the reaction

$$\text{poly(A)} + Mg^{2+} \rightarrow \text{poly(A)} \cdot Mg^{2+} \qquad \text{(d)}$$

it turned out to be impossible to use this difference spectrum for component analysis.

The absorbance dependence upon temperature at 275, 280, 285 and 290 nm after appropriate correction for slight changes in the light scattering were used to calculate the relative proportions of both components making use of the method of least squares.

The fraction of dissociated and disproportionated base triplets f_{kj} as a function of temperature was derived from the system of linear equations

$$f_{kj} = (\beta_{ki} \cdot \beta_{ik})^{-1} \cdot (\beta_{ki} \cdot \Delta A_{ij}) \qquad (3)$$

Here k ($k = 1,2$) refer to the disproportionation and dissociation of the third strand, i and j stand for the wavelength and the temperature, respectively. β_{ki} is a matrix of spectral coefficients which could be found from the difference spectra (a), (b) and (c) using the known concentrations of the components; ΔA_{ij} is the matrix of absorbance differences. Due to linear dependence between the spectra (a), (b) and (c) it is only possible to describe simultaneously any one pair of these reactions.

The same method was applied to describe the difference spectrum accompanying the titration of poly(A) · poly(U) with $MgCl_2$ at 20°C:

$$\text{poly(A)} \cdot \text{poly(U)} + Mg^{2+} = \text{poly(A)} \cdot \text{poly(U)} \cdot Mg^{2+} \qquad \text{(e)}$$

Absorbance differences at 270, 275, 280, 285 and 290 nm were used for calculations.

The method is described in detail in our earlier paper [26].

2.7. Temperature control and recording of melting curves

Heating and cooling cycles between the spectral measurements were used to establish melting curves at 260 nm. The spectrophotometer was equipped with a MK70 Cryostat and an U1 ultrathermostat (MLW Prüfgeräte-Werk, Medingen) for low temperature measurements as well as with an Accuron (Cambridge) SPX876 Series2 Temperature Programme Controller for use at higher temperatures. Special thermostabilized cell holders for both single 1.00 cm and 4.00 cm cells were used together with an ultrathermostat and/or cryostat. In case of 0.50, 1.00 and 4.00 cm cuvettes the temperature sensor was placed directly in the solution under investigation; in case of smaller cuvettes the temperature was measured in the circulating water.

Melting curves were recorded and treated by a personal computer connected to the SP8-150 instrument. The usual rate of temperature change was about 0.4°C/min. Readings of absorbance (four decimal digits) and of temperature with the precision of 0.1°C were taken in intervals of one second and averaged digitally every 0.1°C. Both cooling and heating curves were recorded.

2.8. Calculation of binding constants

Binding constants were calculated according to the formula of McGhee and von Hippel [27]:

$$\frac{\nu}{L} = K \cdot (1 - N\nu) \cdot \left[\frac{(2\omega - 1)(1 - N \cdot \nu) + \nu - R}{2(\omega - 1)(1 - N\nu)}\right]^{N-1} \cdot \left[\frac{1 \quad (N+1)\nu + R}{2(1 - N\nu)}\right]^{2} \qquad (4)$$

$$R = \sqrt{[1 - (N+1)\nu]^2 + 4\omega\nu(1 - N\nu)} \qquad (5)$$

where K is the binding constant (M^{-1}) for isolated binding, ω is a cooperativity parameter, N is the number of base pairs covered by one ligand molecule, L is the concentration of free ligand and ν is the fraction of bound ligands per base pair.

$$L = c_{U,f}/n = (c_{U,t} - c_{U,b})/n \quad (6)$$

$$\nu = (c_{U,b}/n)/(c_{AU,t}/2) \quad (7)$$

$$c_{U,b} = \Delta A_{260}/\Delta\epsilon_{AU+U,260} \quad (8)$$

$c_{U,t}$, $c_{U,f}$ and $c_{U,b}$ are the total concentrations of the oligomer and that of the free and bound fractions, respectively, n characterizes the length of the oligomer, ΔA_{260} is the experimental value of the absorbance difference at 260 nm found according to Eq. (1) or Eq. (2); $c_{AU,t}/2$ is the total concentration of the A · U base pairs of the polymer; $\Delta\epsilon_{AU+U,260}$ is the extinction difference of uridylic residues in free and bound states of oligouridylic acid. Throughout the calculations, a reference value of $\Delta\epsilon_{AU+U,260} = -5700\ l \cdot mol^{-1} \cdot cm^{-1}$ for the association of the third (Hoogsten) strand as derived from our experiments with poly(U) was used. Both ν and L could be derived from the differences of experimental absorbances ΔA_{260} (Eqs. (6) and (7)) and concentrations $c_{U,t}$ and $c_{AU,t}$.

In calculations, N was taken equal to n with the intention to reduce the relative error of the parameters. When all three parameters (K, ω and N) were estimated simultaneously, the value of N was found to be in accordance with the expected value of n within a range of ± 0.6. The data dealing with pentamer [28] were evaluated anew in agreement with other calculations.

2.9. Program ALAU

Binding constants of a series of $(pU)_n$ oligomers were determined using a model-based analysis realized in the program system ALAU [29,30]. This set of programs runs on minicomputers and PCs and serves parameter estimation in nonlinear regression models by the least-squares criterion; the general break-off criterion is the parameter accuracy. As a result of experiences with model-free analysis, the model-specific subroutine for ALAU is written in such a way that different series of measurements can be used simultaneously for the parameter estimation. By that, the program yields the optimum value of $\Delta\epsilon_{AU+U,260}$ besides those for the binding parameters. Thus, only experimental values of absorbances and total concentrations are needed as input data; there is no need to transform the data nor to make additional assumptions concerning the value of $\Delta\epsilon_{AU+U,260}$.

3. Results

3.1. Difference spectra of poly(A) · poly(U) with respect to Mg^{2+} concentration and temperature

The difference spectra from the transfer of both poly(A) · poly(U) and $(pU)_n$ solutions into 10 mM in Mg^{2+} and cooling/heating in the interval 5–45°C were recorded, aiming to obtain undistorted results for differences of absorbance accompanying the complex formation when both the temperature and solute conditions are subjected to change.

Titration of poly(A) · poly(U) solution with $MgCl_2$ results in a difference spectrum with a wide negative peak around 270 nm (Fig. 1a). The depth of the minimum increases rapidly in the range 0.01–1 mM Mg^{2+}. Starting at this point, the behaviour of the difference spectrum changes: instead of the isosbestic point at 285 nm a new isosbestic point appears at 260 nm (Fig. 1b); the positive peak at 290 nm disappears. The deflection point in response to increasing Mg^{2+} concentration on the graphs of absorbance dependences upon Mg^{2+} concentration had been observed earlier on poly(A) · poly(U) [31] as well as on poly(dA) · poly(dT) [32] titration curves.

For quantitative treatment, component analysis was applied to the difference spectra. The experimental difference spectra connected with the transfer of poly(A) · poly(U) into 10 mM $MgCl_2$ (Fig. 1c, curve 1) was resolved into two components by least squares. As components the partial difference spectra of the same reaction were used: (1) 'low magnesium', a difference spectrum recorded upon addition of 0.2 mM $MgCl_2$, and (2) 'high magnesium', a difference spectrum observed upon increasing the $MgCl_2$ concentration from 13.60 to 14.15 mM. Consequently, it became possible to distinguish the components of the composite spectrum (curves 2 and 4, respectively). As a comparison the difference spec-

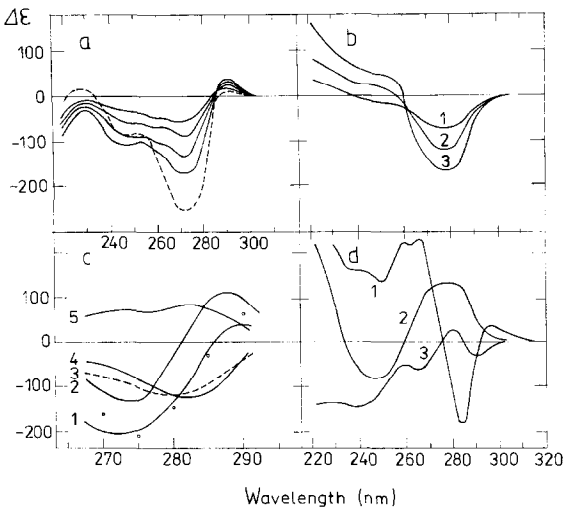

Fig. 1. Titration of poly(A)·poly(U) and $(pU)_n$ with $MgCl_2$ in 1 mM cacodylate buffer (pH 7.0) containing 10 mM NaCl, and respective thermal difference spectra in CNM buffer. Concentration of poly(A)·poly(U), $c_{AU,1} = 0.50.10^{-4}$ M. (a) Titration of poly(A)·poly(U) at 22°C, $MgCl_2$ concentration: (from top to bottom) 0.05 mM, 0.14 mM, 0.49 mM, 1.00 mM, and 10.0 mM (broken line). (b) Titration of poly(A)·poly(U) with $MgCl_2$ (against 1 mM $MgCl_2$): (1) 5.0 mM, (2) 10 mM, (3) 20 mM $MgCl_2$. (c) The results of component analysis. (1) Experimental difference spectrum accompanying the addition of 10 mM Mg^{2+} to the poly(A)·poly(U) solution in 10 mM NaCl at 20°C, ○ – respective values calculated on the basis of spectral components, (2) 'low magnesium' spectral component, (3) difference spectrum of poly(A)·poly(U) disproportionation reaction, ordinate: 0.032·$\Delta\epsilon$, (4) 'high magnesium' spectral component, (5) difference spectrum accompanying the cooling of the poly(A)·poly(U) solution from 20°C to 5°C. The meaning of 'high/low Mg' is explained in Section 3.1. (d) (1) Difference spectrum of poly(A)·poly(U) in the predenaturation range upon heating to 45°C against the spectrum at 5°C in CNM buffer; (2,3) difference spectra of oligouridylic acids: (2) $(pU)_7$ in 1 mM cacodylate buffer containing 10 mM NaCl upon addition of $MgCl_2$, final concentration 10 mM $MgCl_2$; (3) $(pU)_8$ in presence of 10 mM $MgCl_2$ at 5°C against 45°C.

trum of disproportionation reaction is given (dashed line, curve 3).

The difference spectrum of the first component (curve 2) with isosbestic point at 281 nm (in effect, redshift) is definitely unlike to the difference spectrum of the duplex or triplex formation or dissociation. It could be supposed that the spectrum is due to a conformational transition. The difference spectrum in the concentration range over 10 mM Mg^{2+} (curve 4) bears a likeness to the spectrum accompanying the disproportionation (curve 3).

Upon cooling of the solution to 5°C and incubation during 1 h the changes in difference spectrum demonstrate the reverse reaction to take place as evidenced by the curve 5. It could be seen that the changes are similar to those described by curve 4 with opposite sign, i.e. the resulting difference spectrum approaches zero. As calculated from the residual the contamination of the poly(A) · poly(U) specimen with the triple helix does not exceed 3% at 5°C.

However, in the relative scale the changes of the spectra were not very wide when compared to the value of the molar extinction itself ($\epsilon_{260} = 6655$ $l \cdot mol^{-1} \cdot cm^{-1}$). The mean correction $\Delta\epsilon'_{260} = -165$ $l \cdot mol^{-1} \cdot cm^{-1}$ was applied in calculations when the $MgCl_2$ concentration was increased up to 10 mM.

Due to large increase of the light scattering of the solution it was not possible to record the difference spectrum of poly(A) associated with the transfer into 10 mM $MgCl_2$. Instead, the difference spectrum of $(pA)_{12}$ was recorded (not shown). In general, the difference spectrum was quite similar to the difference spectrum observed upon 1:1 interaction of poly(A) with poly(U) on a smaller scale with double minimum at 255 and 264 nm (both $\Delta\epsilon' = -500$ $l \cdot mol^{-1} \cdot cm^{-1}$) and the isosbestic points at 234.5 and 279 nm.

The temperature difference spectrum of a poly(A) · poly(U) solution is depicted in Fig. 1d (curve 1). The difference spectrum in the pre-denaturation range has a minimum at 284 nm and a broad composite maximum at 258–267 nm ($\Delta\epsilon''_{284} = -190$ $l \cdot mol^{-1} \cdot cm^{-1}$, $\Delta\epsilon''_{260} = 215$ $l \cdot mol^{-1} \cdot cm^{-1}$) between 5 and 45°C, with its isosbestic point at 274 nm (all values listed here and below are given without correction to the change of the solution volume upon temperature). Most of these changes take place in the region from 30 to 45°C (Fig. 2a); the changes due to the heating of the solution from 5°C to room temperature are small. The absorbance change in the premelting region shown in Fig. 2a was used to correct the melting curves of the complexes.

These two corrections together (i.e., transfer into Mg^{2+} solution and cooling, $\Delta\epsilon = \Delta\epsilon' + \Delta\epsilon''$) result in a correction of $\Delta\epsilon_{260} = -195$ $l \cdot mol^{-1} \cdot cm^{-1}$, hence, $\epsilon_{AU,260} = 6460$ $l \cdot mol^{-1} \cdot cm^{-1}$ for poly(A) · poly(U) at 5°C in the presence of 10 mM NaCl and 10 mM Mg^{2+}.

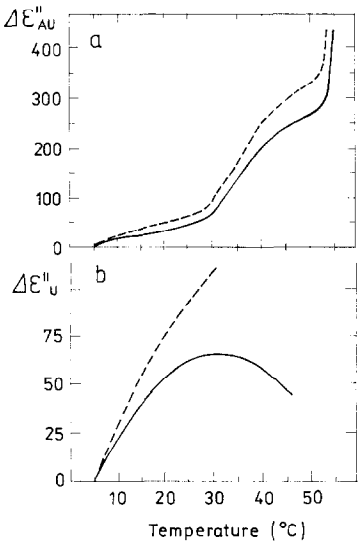

Fig. 2. (a) Initial part of the poly(A)·poly(U) disproportionation/melting curve in CNM buffer as followed at 260 nm. The disproportionation proceeds at 26°C whereas the melting begins at about 55°C; note that the hyperchromicity of the poly(A)·poly(U) solution at the onset of melting is about 4% with respect to the absorbance at 5°C (cf. Fig. 5). (b) Dependence of the extinction ($\Delta\epsilon''_{U,260}$) of $(pU)_{10}$ upon temperature in CNM buffer. For both graph (a) and (b), the data not corrected for the thermal expansion of the solution are shown by the continuous line, the broken line represents corrected data.

3.2. Difference spectra of oligo(U) with respect to Mg^{2+} and temperature

The change in absorbance of uridylic acid oligomers at 260 nm when the solution is made 10 mM with respect to Mg^{2+} is rather small (Fig. 1d, curve 2). The apparent extinction ϵ_{260} of $(pU)_n$ decreases when the temperature is lowered to 5°C (curve 3). Upon heating, the apparent maximum appears in the vicinity of 30°C (Fig. 2b, continuous line). This dependence was similar for all oligomers. The occurrence of the maximum can easily be explained by the interrelation between the real increase of the absorbance and the thermal expansion of the solution: after appropriate correction to thermal expansion the absorbance continues to increase with temperature (Fig. 2b, broken line). However, melting of the complexes was recorded using the single beam mode without temperature correction; therefore, the melting data were corrected in accordance with the initial curve.

3.3. The state of the polymer–oligomer system under the conditions of experiment

The increase of ionic strength is known to result in the stabilisation of the triple helix; the pronounced role of Mg^{2+} ions in this respect is generally accepted. Therefore, a series of experiments were performed to examine the behaviour of poly(A)·poly(U) upon transfer into the solution containing 10 mM MgCl. Decrease of the absorbance at 280 nm during the melting of poly(A)·poly(U) was revealed; this was not the case when complexes were investigated. The hypochromic change at 280 nm as well as the presence of an isosbestic point at 286 nm were taken as spectroscopic evidence of triplex formation [12,33]. The method of least squares was applied in order to find the spectral components associated with the melting transition (cf. Section 2.6).

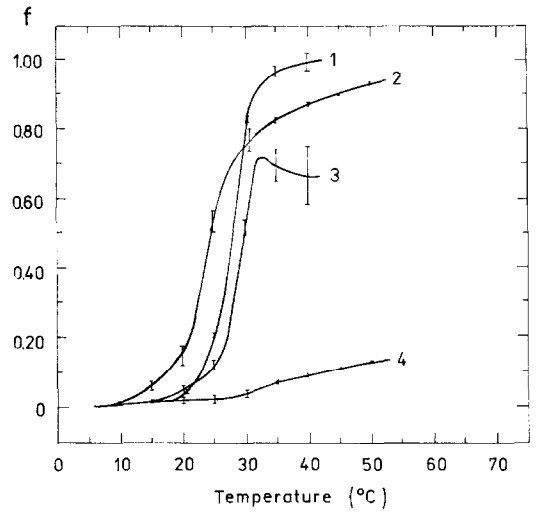

Fig. 3. The results of component analysis. The curves depicting the transitions 2AU → A2U + A (2,3) and A2U → AU + U (1,4) are represented as a function of temperature in CNM buffer. (2,4) poly(A)·poly(U), $c_{AU,t} = 0.32 \cdot 10^{-4}$ M. (1,3) complex of poly(A)·poly(U) with $(pU)_9$, polymer concentration $c_{AU,t} = 0.26 \cdot 10^{-4}$ M, $r = 2.00$. On the ordinate, the fraction of disproportionation/dissociation reaction taken place at particular temperature as calculated from the respective molar difference spectra is shown. To get a proper calibration of curves (coefficients β), concentrations on the basis of phosphorus were multiplied by 0.5 for curves (1) and (4) and 0.25 for curves (2) and (3). Vertical bars for every 5°C show the standard deviations of respective points.

The transition 2poly(A) · poly(U) → poly(A) · 2poly(U) + poly(A) was found to take place between 20 to 30°C with the midpoint at 26°C (Fig. 3). This disproportionation is also associated with a slight dissociation of the triplex beginning at 30°C, possibly due to short or otherwise defective stretches of uridylic acid on the third strand. The double helix is totally converted to triplex as proved by the location of the end of the curve approximately at the level of 100%. It must be deduced that really no triplex was present at temperatures below 10°C. In the case of complexes with oligonucleotides the curve of disproportionation is shifted toward higher temperatures in accordance with dissociation of oligomers. The disproportionation reaction proceeds as the triple strand consisting of uridine oligomers dissociate (Fig. 4b). Both curves are almost parallel (Fig. 3) which means that the sites becoming free from the oligomer are immediately covered by poly(U) (Fig. 4c). The fit of the theoretical curves is notably good, the mean relative error [26] being in the range 0.03% for polymer solution which allows to consider the spectra of just two components suitable to describe the situation adequately. In case of complexes the mean square deviations of the disproportionation reaction increase notably at the very end of the transition, whereas the respective curve seems to be cut off, which lets one suppose that some other reactions could be involved. However, application of $(pA)_{12}$ difference spectrum upon reaction with Mg^{2+} in component analysis did not produce any improvement of the fit in the terminal part of the curves.

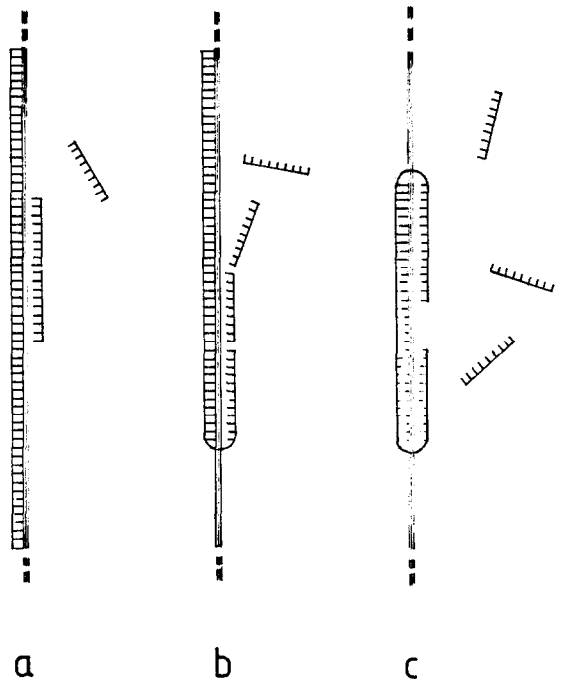

Fig. 4. Structural transitions of oligouridylic acid complex with poly(A)·poly(U) as a function of temperature. (a) Double helix poly(A)·poly(U) at 5°C covered by uridine oligomers as a third strand, (b) two transitions taking place simultaneously at 25°C: disproportionation of poly(A)·poly(U) and dissociation of $(pU)_n$, (c) at 30°C, disproportionation reaction of poly(A)·poly(U) is almost completed, uridine oligomers unbound. Thick line represents poly(A) strand, whereas thin lines are used for poly(U). Hydrogen bonding between poly(A) and poly(U) strands having Watson–Crick and Hoogsten pairing schemes is shown by full-length and shortened lines respectively.

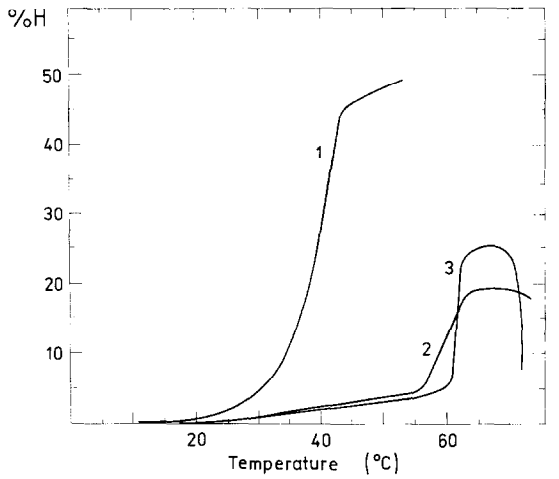

Fig. 5. Disproportionation/melting curves of (1) poly(A)·poly(U) at 260 nm in 1 mM cacodylate buffer (pH 7.00) containing 10 mM NaCl, (2) the same, containing both 10 mM NaCl and 10 mM $MgCl_2$ (CNM buffer); (3) melting of poly(A)·2poly(U) in CNM buffer.

When the melting of poly(A) · poly(U) specimen (A:U = 1:1) is followed at 260 nm the main transition begins at 55°C (Fig. 5, curve 2). These changes could possibly be interpreted as a dissociation of the triple helix poly(A) · 2poly(U) which was formed between 20 and 30°C. The dissociation is accompanied by a simultaneous formation of the initial double helix and aggregation/precipitation of the complex as monitored by an increase of turbidity due to the presence of Mg_{2+} ions. Melting of the triple

helix poly(A) · 2poly(U) (A:U = 1:2) under the same conditions begins at 61°C and is highly cooperative (curve 3). The jump in hyperchromicity due to dissociation of the intermediate structures (probably, of double helices) formed at 60–65°C proceeds at 84°C in both cases. Small differences in the initial part of the melting curve at 55°C could be due to the non-equilibrium state of the triple helix formed from the original poly(A) · poly(U) double helix during the transition at 26°C.

Otherwise, the disproportionation reaction could not be followed at 260 nm, but a very small increase in absorbance (about 1% increase of hyperchromicity at 30°C, Fig. 3) would appear. There is a marked increase of absorbance in the interval between 30 and 50°C (4% hyperchromicity at 50°C) which could be connected with the unstacking of poly(A) in presence of Mg_{2+} and/or dissociation of short stretches of poly(U).

The conclusion that at 5°C the poly(A) · poly(U) in presence of 10 mM $MgCl_2$ is free of triple helix could be drawn. This is based on the following experimental data: (1) component analysis of difference spectra (Fig. 1c), (2) component analysis of the melting curves (Fig. 3), (3) titration of poly(A) · poly(U) with poly(U) (see Section 3.4).

However, the triplex structure is present at temperatures beginning from 20°C and higher and this is why the melting temperatures themselves could not be used to calculate the thermodynamic parameters. On the other hand, the absorbance at 260 nm (isosbestic point of the disproportionation reaction is at 261 nm) is almost not affected by the reaction. Moreover, when the absorbance curves are corrected for changes taking place in poly(A) · poly(U) in the same region, the net change of ΔA_{260} could solely be assigned to the dissociation of oligo(U).

3.4. Difference spectra of the complexes of poly(A) · poly(U) with poly(U) and uridylic acid oligomers

The temperature of disproportionation close to room temperature makes it necessary to appreciate the possible presence of triple helix in poly(A) · poly(U) specimens at reference temperature (5°C). It is complicated to check the possible presence of triple helix directly. However, the presence of triplex

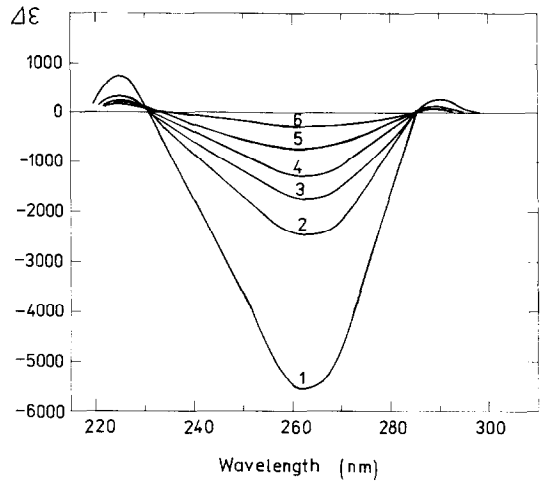

Fig. 6. Thermal difference spectra of the complexes of poly(U) and $(pU)_9$ with poly(A) · poly(U) accompanying the association of the third strand in CNM buffer. (1) Difference spectrum related to the association of poly(U) with the double helix poly(A) · poly(U). Curves (2)–(6): difference spectra of the complexes poly(A) · poly(U) + $(pU)_9$. The concentration of the polymer, $c_{AU,t} = 0.42 \cdot 10^{-4}$ M. The ratio $r = [P^-]_{oligo(U)}/[P^-]_{poly(A \cdot U)}$ was as follows: (2) 1.00, (3) 0.40, (4) 0.30, (5) 0.11, (6) 0.07.

is expected to manifest itself by the equal concentration of free poly(A) in the specimen.

Titrations of poly(A) · poly(U) solution with poly(U) were used for this purpose, since the value of the isosbestic point is believed to be a good indicator of the binding peculiarities. It turned out that at the very beginning of titration the isosbestic point of the difference spectrum was shifted slightly towards shorter wavelengths as compared to the expected value 286 nm; this shift is indicative of simultaneous formation of the double and triple helices. For quantitative estimation of the relative amount of triplex present, difference spectra were calculated for formation of triple and double helices in different proportions. The expected shift of the isosbestic point was found as a function of the composition of the specimen. It proved to be the case that there was no more than 3.5% free poly(A) present in our specimens at 17°C.

Fig. 6, curve 1 shows that the interaction of poly(U) with the poly(A) · poly(U) double helix in presence of Mg^{2+} results in a difference spectrum with a minimum at 262 nm, and an isosbestic point at 286 nm as expected [12,33]; $\Delta\epsilon_{AU+U,260} = -5700$ $l.mol^{-1} \cdot cm^{-1}$. The difference spectra obtained after

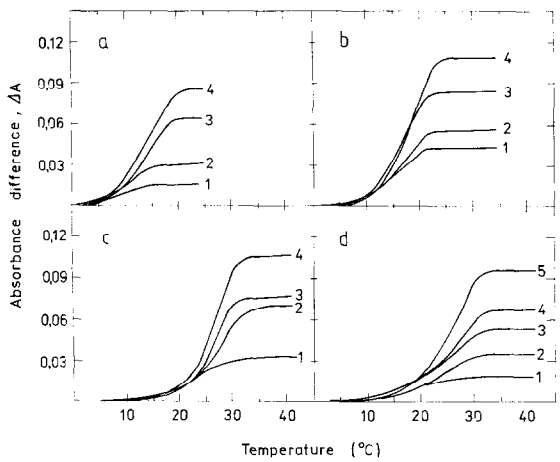

Fig. 7. Typical melting curves for oligo(U) complexes with poly(A)·poly(U) in CNM buffer; all curves were corrected for poly(A)·poly(U) absorbance increase in the same region. (a) $n = 7$, $c_{AU,t} = 0.435–0.446 \cdot 10^{-4}$ M. (1) $r = 0.10$, (2) $r = 0.22$, (3) $r = 0.50$, (4) $r = 0.68$; (b) $n = 8$, $c_{AU,t} = 0.116–0.137 \cdot 10^{-4}$ M, (1) $r = 0.19$, (2) $r = 0.27$, (3) $r = 0.48$, (4) $r = 0.58$; (c) $n = 9$, $c_{AU,t} = 0.335–0.402 \cdot 10^{-4}$ M. (1) $r = 0.20$, (2) $r = 0.49$, (3) $r = 0.60$, (4) $r = 0.79$; (d) $n = 10$, $c_{AU,t} = 0.103–110 \cdot 10^{-4}$ M, (1) $r = 0.15$, (2) $r = 0.22$, (3) $r = 0.31$, (4) $r = 0.42$, (5) $r = 0.60$.

cooling of the complex of poly(A)·poly(U) with $(pU)_9$ are represented by curves 2–6. These difference spectra are similar to those observed in the case of poly(U) including the position of isosbestic points; the value of 286 nm is assumed to be specific for binding of the third strand. The hypochromicities depended upon input ratio r in expected manner and the absorbance differences at 260 nm were used to estimate the binding parameters.

The reaction was completed almost immediately after cooling; only small changes of absorbance took place in the cuvette with the poly(A)·poly(U) + oligo(U) complex during the first hour after 5°C had been reached. One hour was the standard time before beginning the measurement of the spectrum at 5°C and the melting experiment thereafter. Generally speaking, there was no further decrease of absorbance on a prolonged period of cooling, except for the case of the shortest oligonucleotides.

The details concerning experiments with pentauridylic acid have been presented in an earlier report [28].

3.5. Melting of the complexes

In all cases the dissociation of complexes of uridylic acid oligomers ($n = 7–10$) anticipate or go parallel with the disproportionation reaction of the double helix (Fig. 3). These reactions, in turn, precede the onset of poly(A)·2poly(U) melting (Fig. 7, cf. Fig. 5). Consequently, in the temperature interval under investigation, the hyperchromicities associated with the dissociation of uridylic acid oligomers could be estimated independently of the contribution of the melting of polymer double and triple helices. Small corrections for the change in poly(A)·poly(U) and $(pU)_n$ absorbance with respect to temperature in the predenaturation region accounts for disproportionation and small changes in stacking, conformation and/or partial dissociation. For some of the experiments, the melting temperatures of the complexes plotted against ratio r are shown in Fig. 8.

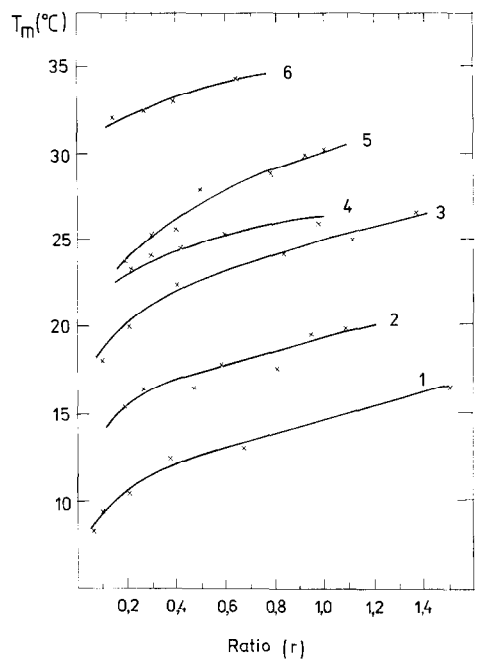

Fig. 8. Melting temperatures of the complexes of uridylic acid oligomers with the poly(A)·poly(U) double helix in CNM buffer as a function of input ratio (r). Curves are depicted for $n = 7 – 10$; the concentration of polynucleotide varies within the limits given below: (1) $n = 7$, $c_{AU,t} = 0.363–0.558 \cdot 10^{-4}$ M, (2) $n = 8$, $c_{AU,t} = 0.116–0.167 \cdot 10^{-4}$ M, (3) $n = 9$, $c_{AU,t} = 0.093–0.106 \cdot 10^{-4}$ M, (4) $n = 10$, $c_{AU,t} = 0.103–0.113 \cdot 10^{-4}$ M, (5) $n = 9$, $c_{AU,t} = 0.424–0.449 \cdot 10^{-4}$ M, (6) $n = 10$, $c_{AU,t} = 0.865–0.872 \cdot 10^{-4}$ M.

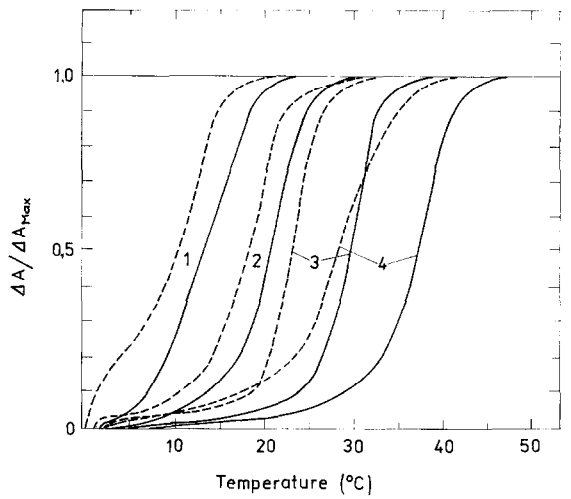

Fig. 9. Normalized absorbance vs. temperature accompanying the association/dissociation of the complexes of uridylic acid oligomers with poly(A)·poly(U) ($c_{AU,t} = 0.43 \cdot 10^{-4}$ M) upon cooling and heating in CNM buffer: (1) $n = 7$, $r = 0.68$; (2) $n = 8$, $r = 0.40$; (3) $n = 9$, $r = 0.93$; (4) $n = 10$, $r = 0.75$. Heating curves are shown by continuous lines, for cooling curves broken lines are used. All curves were corrected for the poly(A)·poly(U) absorbance increase in the depicted region.

In order to follow the hysteresis accompanying the cyclic heating and cooling, several experiments with uridylic acid nanomers and decamers were performed using the initial heating of the solutions up to 45°C, subsequent cooling and heating again. Spectral changes induced by the initial heating were not fully reversible. Therefore, most of the regular experiments were performed without the initial heating/cooling cycle. All (heating)–cooling–heating curves revealed appreciable hysteresis (Fig. 9).

It is perhaps too sophisticated a task to describe in detail the possible transition of the polymer–oligomer system during the heating and cooling cycles. It seems possible that after the first heating and cooling poly(A)·poly(U) transforms into and retains the triple helical structure (at least partly) if excess of uridine oligomers is present whereas the interaction of oligomers takes place with free poly(A). Thus, the second heating cycle possibly represents the dissociation of uridylic acid oligomers partly from the complex with poly(A) and not from the poly(A)·poly(U).

3.6. Scatchard representation of the data

For preliminary analysis of the data, binding isotherms in Scatchard representation were used. The graph for $(pU)_7$ as an example is depicted in Fig. 10. The points are located on a convex curve typical for

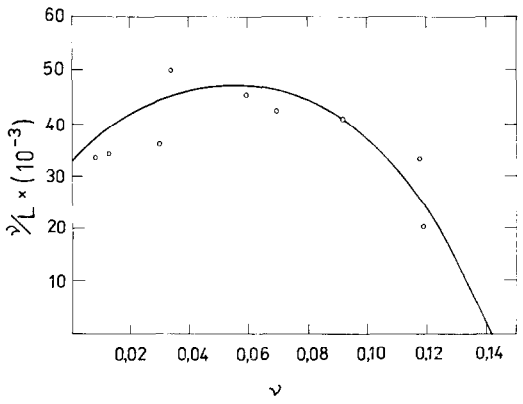

Fig. 10. The binding of $(pU)_7$ to double helical poly(A)·poly(U) in the Scatchard representation. Horizontal axis, the number of bound oligomer molecules per base pair of the double helix, $\nu = (c_{U,b}/n)/(c_{AU,t}/2)$; vertical axis, $\nu/L = \nu/(c_{U,f}/n)$. The parameters found from the ALAU calculations ($K = 0.55 \cdot 10^6$ M^{-1}, $\omega = 16.9$) were used to plot the curve; the number of base pairs covered by one ligand molecule (N) is supposed to be 7.00, $\Delta\epsilon_{AU+U,260} = -5700$ l·mol^{-1}·cm^{-1}.

Table 1
Binding parameters of uridylic acid oligomers in 1 mM cacodylate buffer pH 7.0 containing 10 mM NaCl and 10 mM $MgCl_2$ (CNM buffer)

n	$K_{c,n}$ [a]	ω_n	ΔG_c^{0} [b]	$\Delta G_c^{0}/n$ [c]
5	30700±600	44.0±4.0	−5.70±0.01	−0.77
	29500±1300 [d]			
7	0.55(±0.02)·10^6	16.9±2.3	−7.30±0.02	−0.78
	0.57(±0.02)·10^6 [d]			
8	2.96(±0.53)·10^6	19.0±7.5	−8.23±0.10	−0.80
	2.82(±0.44)·10^6 [d]			
9	5.33(±0.18)·10^6	37.3±6.1	−8.55±0.02	−0.74
	5.10(±0.24)·10^6 [d]			
10	12.60(±1.22)·10^6	22.8±7.4	−9.02±0.05	−0.72
	12.56(±1.11)·10^6 [d]			
	(weighted mean)	24.5±5.6		−0.76

[a] Binding constant (M^{-1}) for contiguous binding.
[b] Free energy per mole of oligonucleotide, kcal·mol^{-1} (contiguous binding).
[c] Free energy per mole of uridine residue, kcal·mol^{-1} (binding to isolated site).
[d] Binding constants as recalculated for mean value of $\omega = 24.5$.

cooperative binding. However, the binding parameters were not directly calculated from this graph by least squares because biased values would be obtained owing to unequal statistical weights of the points.

3.7. Binding parameters

The binding data are presented in Table 1. The parameters were calculated by way of least squares using the computer program ALAU; the values of N in Eqs. (4) and (5) were taken to be equal to the length of the respective oligomer n ($N = n$), $\Delta\epsilon_{AU+U,260} = -5700\ l \cdot mol^{-1} \cdot cm^{-1}$. The binding parameters for the pentamer were recalculated from the data [28], in accordance with the calculations used for other oligomers.

Upon increasing the length of oligomer, the contiguous binding constant, $K_{c,n} = K_n \cdot \omega_n$, increases from 30700 ($n = 5$) up to $12.6 \cdot 10^6\ M^{-1}$ for $n = 10$, whereas the cooperativity coefficient did apparently not depend on the oligomer length. In Fig. 11, the dependence of $\Delta G^0_{c,n}$ upon n is depicted. Linear approximation yields a value of 0.72 (± 0.03) for the slope; this value (in kcal · mol^{-1}) is equal to the free energy $-\Delta G^0_{c,U}$ of the contiguous binding per uridylic acid residue to the poly(A) · poly(U) double helix in Hoogsten position. Using the mean value of the cooperativity parameter $\omega = 24.5$, a free energy value of $\Delta G^0_{c,U} = -0.69(\pm 0.05)$ kcal · mol^{-1} is found.

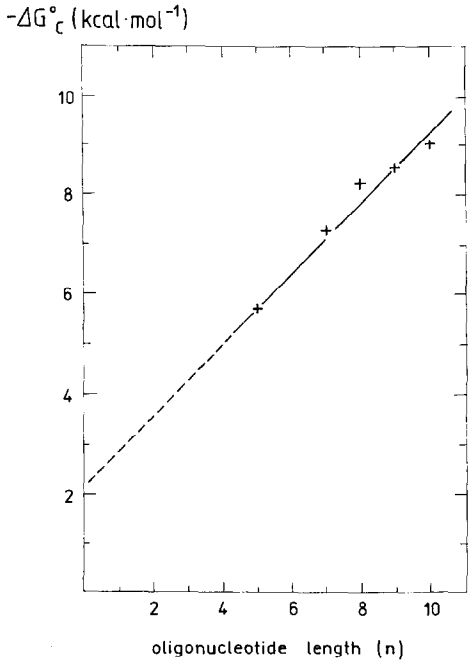

Fig. 11. Free energy of contiguous binding ($-\Delta G^0_c$, kcal · mol^{-1}) of uridylic acid oligomers to double stranded poly(A) · poly(U) vs. length of the oligonucleotide (n) measured in 1 mM cacodylate buffer pH 7.0 containing 10 mM NaCl and 10 mM $MgCl_2$. On the X-axis is the length of the oligomer, on the ordinate the free energy (see Table 1). The data are approximated by the linear regression $-\Delta G^0_c = 2.14 + 0.72 \cdot n$.

4. Discussion

The model used assumes a binding to an infinite homogeneous polymer with overlapping potential binding sites. We have to discuss its applicability to measurements of finite-lengths polymers. It is a well-accepted criterion that the polymer length should be large in comparison with the mean length of occupied (or unoccupied) regions at half saturation (N(b)). To check this, we have reformulated the model in dependence on a nucleation parameter. By logarithmic derivation of the partition function with respect to this parameter, one can get the mean length of these regions. For the parameters given in Table 1 we obtained the following values for N(b): 17.97, 15.28, 17.32, 23.75, and 21.24. Since the lengths of poly(A) · poly(U) double helices are broadly distributed in the range 50–500 bp (with an estimated mean length of 200 bp), the application of the model is justified.

The monitoring of the changes of hypochromicity in the 260 nm band accompanying the complex formation of nucleic acids with ligands has not been used so far for the characterization of the thermodynamic properties of the complexes. In the case of oligonucleotides the complex formation with a double helix is accompanied by hypochromic change; this change has been exploited in the present work to calculate the binding parameters and free energy of interaction. Using oligouridylic acids of different length, it became possible to determine the free energy of binding per uridylic acid residue upon triple helix formation as well as the free energy of cooperative interaction of oligomers. We assume that

amongst the conditions of the experiment performed there were no competitive processes interfering with the complex formation. There is no reason to suspect the presence of intermediate states during the complex formation as well. We suppose therefore that the present method does not suffer from the shortcomings related to the method of thermal denaturation as well as other possible causes for the following reasons:

First, uridylic acid oligomers, unlike poly(U) [34,35], do not reveal any appreciable secondary structure in the presence of 10 mM Mg^{2+} at temperatures close to 0°C (Fig. 1d). Poly(U) is supposed to form a stacked or double stranded structure at temperatures below 10°C in the presence of Mg^{2+} [36,37]; the double stranded structure could be formed by folding of the molecule [35].

Second, there is no free poly(A) in the solution at the temperatures of the present experiment. Poly(A) and oligo(A) are known to form extensive secondary structure in the presence of Mg^{2+} ions [38]. However, poly(A) in our case becomes only free after disproportionation of poly(A) · poly(U) which happens at higher temperature, well out of the temperature range used for parameters estimation.

Third, it has been shown [39] that dissociation of the third strand is not accompanied by any significant change in the conformation of the poly(A) · poly(U) double helix. In our conditions of experiment poly(A) · poly(U) assumes a triplex structure at 30°C and therefore interferes with the data concerning the dissociation temperatures of oligomers. However, (i) the absorbance differences at 260 nm accompanying the disproportionation of poly(A) · poly(U) are notably small, (ii) moreover, these small absorbance differences are corrected by the reference values of the free poly(A) · poly(U) in the same region.

Fourth, values obtained using the transition curves could be checked against values found from the expected absorbances at 5°C.

It follows that the method is expected to be almost free of shortcomings when compared with the methods that make use of T_m values for calculations.

Both oligo(U) and oligo(A) and respective polymers have been used earlier to form double and a triple helices [40]. It was found that uridine oligomers as short as pentamer could form a triple stranded helix with poly(A) · poly(U) in the presence of Mg^{2+} in the concentration range of 0.1 to 1.0 mM [P^-] [28]. Hence, it is possible to use relatively short oligomers for the estimation of thermodynamic parameters. For the reasons given above there is no need for significant corrections of the data for conformational transitions, except for small corrections discussed under Sections 2 and 3.

Free energy values were obtained from the respective binding constants given in Table 1 according to the formula

$$-\Delta G^0_{c,n} = RT \cdot \ln(K_{c,n}) = RT \cdot \ln(K_n \cdot \omega_n) \qquad (9)$$

and plotted against the length of oligonucleotides (n) (Fig. 11), as the regression:

$$-\Delta G^0_c = a + b \cdot n \qquad (10)$$

In these formulae, $K_{c,n} = K_n \cdot \omega_n$ is the contiguous binding constant of the oligonucleotide of the length n, and $\Delta G^0_{c,n}$ is the respective free energy. From the weighted least squares approximation, coefficients $a = 2.14(\pm 0.18)$ kcal · mol^{-1} and $b = 0.72(\pm 0.03)$ kcal · mol^{-1} were found. The last figure represents the free energy change per residue upon the contiguous binding of uridylic acid oligomers in Hoogsten pairing with RNA homopolymer.

The values of cooperativity parameters ω_n in our experiments were scattered over the range of 16.9 to 44.0. It seems therefore reasonable to use the weighted mean value of the cooperativity parameter $\omega = 24.5$ (± 5.6) instead of the individual values. The mean difference of free energy between the contiguous (ΔG^0_c) and single binding (ΔG^0_s) for uridylic acid oligomers of $n = 5$–10 is

$$\begin{aligned}\Delta G^0_\omega &= \Delta G^0_c - \Delta G^0_s \\ &= -RT \cdot \ln(K \cdot \omega) + RT \cdot \ln(K) \\ &= -RT \cdot \ln(\omega) = -1.74(\pm 0.13)\ kcal \cdot mol^{-1}\end{aligned} \qquad (11)$$

which is close to the value of the absolute term of linear regression $a = 2.14$ (± 0.18) kcal · mol^{-1}. Respective coefficients of linear regression, calculated on the basis of the mean value of cooperativity parameter ($\omega = 24.5$) and respective values of binding constants, have slightly higher deviations, $a = 2.33$ (± 0.34) kcal · mol^{-1} and $b = 0.69$ (± 0.05) kcal · mol^{-1}

The same energy of interaction between the oligo-

nucleotides has been found in case of cooperative binding of pyrimidine oligodeoxynucleotides located in the neighbouring DNA polypurine sites [41]. The binding free energy of 11-mer oligonucleotides of the composition (dT_9, dC_2) and (dT_8, dC_3) was changed by -1.8 (± 0.3) and -2.1 (± 0.2) kcal · mol^{-1}, respectively, in the presence of another oligonucleotide in the neighbouring site. In the case of DNA double helix the cooperativity is of the same order [42].

It follows that the free energy increment due to cooperativity of interaction is the same for DNA and RNA triple helices of the py · pu · py type. At the same time, the presence of the methyl group of thymine is expected to increase the free energy of interaction as compared with uridine; the same is believed to happen with cytidylic residues. This phenomenon has been known for a long time with respect to double helical polynucleotides [10,40] but was shown to also take place in the case of triple helices [43]. Triplexes formed by oligodeoxyribonucleotides containing methylated or brominated deoxyuracils and methylated deoxycytidines have greater affinities as compared with their unmodified counterparts [44]. Replacement of five cytidine residues with 5-methylcytosine residues affords a stabilization of the triple helix by $-0.1 \ldots -0.4$ kcal · mol^{-1} [45].

It have also been pointed out [41] that the cooperativity effect of oligodeoxynucleotide interaction is not due to the propagation of some conformational transition along the double helix to the adjacent sites as a result of oligonucleotide binding.

Therefore, in order to have the free energy of cooperative interaction equal in both cases (U/U versus dT/dT, both roughly about -2 kcal · mol^{-1}), the RNA Hoogsten strand must have another advantage, perhaps due to the conformation of the RNA residues. A possible explanation could be found in the conformational dissimilarity of DNA [46,47] and RNA [48–50] triple helices (B and A conformations, respectively). It could be assumed that the expected smaller stacking energy of U/U interaction between oligonucleotide joints in the third strand is compensated by a more favourable interaction of pyrimidine bases in the case of RNA triplex as compared with that of the DNA.

Advantages of the cooperative binding of oligonucleotides over the binding to isolated sites have been used in order to enhance the binding affinity and specificity of the triplex formation [51–53].

The earlier data about thermodynamic parameters of A · U base pairs and A · 2U base triplets came mostly from microcalorimetric investigations of homopolymers. The result of our free energy determination for the A · 2U triplex compares well with the data published earlier. Microcalorimetric measurements have supplied the value for free energy of transition $\Delta G^0_{AU} = -1.8$ (± 0.2) and $\Delta G^0_{A2U} = -2.5$ (± 0.3) kcal · mol^{-1} at 25°C for the double and triple helices, respectively from one side, and random coil conformations of the components, from the other [54]. The difference between these values i.e. -0.7 (± 0.5) kcal · mol^{-1} (or about -1.0 kcal · mol^{-1} at 5°C) per ribouridylic acid residue is a respective estimate for the dissociation of the third poly(U) strand.

In order to compare the free energy data for different oligonucleotides, the mean value of the free energy of interaction per nucleotide of the third strand could be found as a quotient $\Delta G^0 = \Delta G^0_s / n$ from respective single oligomer binding data as a rough approximation. In our case, the mean value of $\Delta G^0_s = -0.76$ kcal · mol^{-1} is found for oligoribouridylic acids with $n = 7$–10. As a rule, the free energy values found for dT residues in a third strand in complex with DNA or respective double helical oligonucleotide are a little lower when compared with the ribopolymer data presented here.

In the case of oligothymidylates ($n = 17$, two dC residues), the free energy per Hoogsten interaction of $\Delta G^0 = -0.62$ kcal · mol^{-1} was found by a quantitative DNase I footprint titration at 25°C [55]. An oligonucleotide ($n = 15$) containing both dT and dC (10 and 5 residues, respectively) has free energy values of -0.59 to -0.65 kcal · mol^{-1} per Hoogsten interaction at 8°C, depending on the presence of NaCl/KCl, $MgCl_2$, and spermine [45,56], or -0.60 to -0.72 kcal · mol^{-1} at 24°C [57] for shorter oligonucleotides. These results were found for an isolated binding site of the pyrimidine oligomer on the 438 or 339 bp duplex using the same method. The value of $\Delta G^0 = -0.56$ kcal · mol^{-1} was found for the triple helix formation of dT_{19} with $dA_{19} \cdot dT_{19}$ at 5°C as recalculated from the microcalorimetry data [58] whereas the free energy as calculated for the oligo-

nucleotide of the composition (dT_{10}, dC_5) from other calorimetric data [59] yielded only $\Delta G^0 = -0.22$ kcal · mol^{-1} at the same temperature. However, the data [41] as represented per residue in Hoogsten pairing yielded $\Delta G_s^0 = -0.75$ (± 0.02) kcal · mol^{-1} and $\Delta G_c^0 = -0.91$ (± 0.02) kcal · mol^{-1} at 24°C for single and cooperative binding, respectively, i.e. more than in case of our RNA triple helix experiments.

The free energy values of triple helix formation by oligonucleotides with altered backbone are of the same order. For instance, the triple helix, formed between double stranded plasmid DNA restriction 19 fragment and oligo(dT, $dC)_{17}$ (with just two cytidine residues) containing diastereomeric mixture of phosphothioate linkages as a third strand yields $\Delta G^0 = -0.62$ kcal · mol^{-1} per Hoogsten pairing of the third strand at 25°C [55].

However, due to the diversity of methods, application of oligonucleotides (occasionally containing the cytidine residues), polynucleotides and DNA for experiments, different modifications, temperature and solution conditions etc., it is difficult to draw a solid conclusion from the referred data relevant to RNA/DNA energetics in the triple helix. It is known that RNA and DNA triple helices of mixed composition have quite different conformations as evidenced by CD [60], FTIR [61] and NMR spectra [20]. It is not surprising therefore to find that triplexes differ in stability as well [16–19,61,62]. However, almost all of the authors agree that the most stable triplex is formed by double stranded DNA complexed with the Hoogsten paired RNA strand, whereas RNA double helix complexed with the third RNA strand has much lower stability. It seems that when the applications are considered involving the complexes with DNA double helices, the RNA oligomers have definite advantages over the oligodeoxynucleotides.

Acknowledgements

This work was supported by grant no. 116 from the Estonian Science Foundation to E.R. and K.K. The authors are indebted to Dr. O. Toompuu for critical reading of the manuscript, to Dr. A. Kuusksalu for the electrophoresis of poly(A) · poly(U), and to Dr. Ü. Vaher for help in calculations.

References

[1] L.J. Maher, Bioessays 14 (1992) 807.
[2] P. Hsieh, C.S. Camerini-Otero, R.D. Camerini-Otero, Genes Develop. 4 (1990) 1951.
[3] A. Dayn, G.M. Samadashwily, S.M. Mirkin, Proc. Natl. Acad. Sci. USA 89 (1992) 11406.
[4] C. Hélène, Anti-Cancer Drug Design 6 (1991) 569.
[5] J.-S. Sun, C. Hélène, Curr. Opin. Struct. Biol. 3 (1993) 345.
[6] C. Hélène, J.-J. Toulm, in: J.S. Cohen (Ed.), Oligonucleotides: Antisense Inhibitors of Gene Expression, CRC Press, Boca Raton, 1989, p. 137.
[7] Y.-K. Cheng, B.M. Pettitt, Progr. Biophys. Mol. Biol. 58 (1992) 225.
[8] G.E. Plum, D.S. Pilch, S.F. Singleton, K.J. Breslauer, Ann. Rev. Biophys. Biomol. Struct. 24 (1995) 319.
[9] M.D. Frank-Kamenetskii, S.M. Mirkin, Annu. Rev. Biochem. 64 (1995) 65.
[10] A.M. Michelson, J. Massoulié, W. Guschlbauer, Progr. Nucl. Acid Res. Mol. Biol. 4 (1967) 83.
[11] G. Felsenfeld, T. Miles, Ann. Rev. Biochem. 36 (1967) 407.
[12] C.L. Stevens, G. Felsenfeld, Biopolymers 2 (1964) 293.
[13] M. Riley, B. Maling, J. Chamberlin, J. Mol. Biol. 20 (1966) 359.
[14] A.R. Morgan, R.D. Wells, J. Mol. Biol. 37 (1968) 63.
[15] M.-T. Sarocchi-Landousy, B. Haas, W. Guschlbauer, Biochemistry 16 (1977) 5414.
[16] C. Escudé, J.-C. François, J.S. Sun, G. Ott, M. Sprinzl, T. Garestier, C. Hélène, Nucl. Acids Res. 21 (1993) 5547.
[17] H. Han, P.B. Dervan, Proc. Natl. Acad. Sci. USA 90 (1993) 3806.
[18] S. Wang, E.T. Kool, Nucl. Acids Res. 23 (1995) 1157.
[19] R.W. Roberts, D.M. Crothers, Science 258 (1992) 1463.
[20] J.A. Holland, D.W. Hoffman, Nucl. Acids Res. 24 (1996) 2841.
[21] G.A. Soukup, A.D. Ellington, L.J. Maher, J. Mol. Biol. 259 (1996) 216.
[22] J.U. Skoog, L.J. Maher, Nucl. Acids Res. 21 (1993) 2131.
[23] G.E. Plum, K.J. Breslauer, J. Mol. Biol. 248 (1995) 679.
[24] S.K. Vasilenko, N.A. Serbo, A.G. Veniyaminova, L.G. Boldyreva, V.G. Budker, N.D. Kobetz, Biokhimiya 41 (1976) 260.
[25] G.D. Fasman (Ed.), Handbook of Biochemistry and Molecular Biology, third ed. vol. 1 Nucleic Acids, CRC press, Cleveland, Ohio, 1975, p. 603.
[26] T. Räim, T. Anupõld, E. Raukas, J. Lilles, Mol. Biologiya (USSR) 14 (1980) 94.
[27] J.D. McGhee, P.H. von Hippel, J. Mol. Biol. 86 (1974) 469.
[28] E. Raukas, K. Kooli, V. Yamkovoi, Proc. Estonian Acad. Sci. Chem. 42 (1993) 124.
[29] H. Schütz, E. Stutter, K. Weller, I. Petri, Stud. Biophys. 104 (1984) 23.
[30] E. Stutter, H. Schütz, H. Berg, in: J.W. Lown (Ed.), Anthracycline and Anthracenedione-based Anticancer Agents, Bioactive Molecules, vol. 6, Elsevier, Amsterdam, 1988, p. 245.

[31] V. Buckin, H. Tran, V. Morozov, L.A. Marky, J. Am. Chem. Soc. 118 (1996) 7033.
[32] M. Durand, S. Peloille, N.T. Thuong, J.C. Maurizot, Biochemistry 31 (1992) 9197.
[33] R.D. Blake, J. Massoulie, J.R. Fresco, J. Mol. Biol. 30 (1967) 291.
[34] M.N. Lipsett, Proc. Nat. Acad. Sci. USA 46 (1960) 445.
[35] J.C. Thrierr, M. Dourlent, M. Leng, J. Mol. Biol. 58 (1971) 815.
[36] A.M. Michelson, C. Monny, Proc. Natl. Acad. Sci. USA 56 (1966) 1528.
[37] J. Bandekar, G. Zundel, Biopolymers 23 (1984) 2623.
[38] D. Pörschke, Nucl. Acids Res. 6 (1979) 883.
[39] T. O'Connor, M. Bina, J. Biomol. Struct. Dyn. 2 (1984) 615.
[40] A.M. Michelson, C. Monny, Biochim. Biophys. Acta 149 (1967) 107.
[41] N. Colocci, M.D. Distefano, P.B. Dervan, J. Am. Chem. Soc. 115 (1993) 4468.
[42] O.S. Fedorova, A. Adeenah-Zadah, D.G. Knorre, FEBS Lett. 369 (1995) 287.
[43] J.S. Lee, M.L. Woodsworth, L.J.P. Latimer, A.R. Morgan, Nucl. Acids Res. 12 (1984) 6603.
[44] T.J. Povsic, P.B. Dervan, J.Am. Chem. Soc. 111 (1989) 3059.
[45] S.F. Singleton, P.B. Dervan, Biochemistry 31 (1992) 10995.
[46] K. Liu, H.T. Miles, K.D. Parris, V. Sasisekharan, Nature Struct. Biol. 1 (1994) 11.
[47] G. Ragunathan, H.T. Miles, V. Sasisekharan, Biochemistry 32 (1993) 455.
[48] S. Arnott, P.J. Bond, Nature New Biol. 244 (1973) 99.
[49] R. Raghunathan, H.T. Miles, V. Sasisekharan, Biopolymers 36 (1995) 333.
[50] R. Klinck, J. Liquier, E. Taillandier, C. Gouyette, T. Huynh-Dinh, E. Guittet, Eur. J. Biochem. 233 (1995) 544.
[51] S.A. Strobel, P.B. Dervan, J. Am. Chem. Soc. 111 (1989) 7286.
[52] N. Colocci, P.B. Dervan, J. Am. Chem. Soc. 116 (1994) 785.
[53] M.D. Distefano, P.B. Dervan, Proc. Natl. Acad. Sci. USA 90 (1993) 1179.
[54] E. Neumann, T. Ackermann, J. Phys. Chem. 73 (1969) 2170.
[55] J.G. Hacia, B.J. Wold, P.B. Dervan, J. Am. Chem. Soc. 33 (1994) 5367.
[56] S.F. Singleton, P.B. Dervan, J. Am. Chem. Soc. 116 (1994) 10376.
[57] S.F. Singleton, P.B. Dervan, J. Am. Chem. Soc. 114 (1992) 6957.
[58] H.P. Hopkins, D.D. Hamilton, W.D. Wilson, G. Zon, J. Am. Chem. Soc. 97 (1993) 6555.
[59] G.E. Plum, Y.-W. Park, S.F. Singleton, P.B. Dervan, K.J. Breslauer, Proc. Natl. Acad. Sci. USA 87 (1990) 9436.
[60] H.T. Steely, D.M. Gray, R.L. Ratliff, Nucl. Acids Res. 14 (1986) 10071.
[61] C. Dagneaux, J. Liquier, E. Taillandier, Biochemistry 34 (1995) 16618.
[62] J. Liquier, E. Taillandier, R. Klinck, E. Guittet, C. Gouyette, T. Huynh-Dinh, Nucl. Acids Res. 23 (1995) 1722.